

Closed form approximation of the actual spectral power emission of commercial color LEDs for VLC

Alexis A. Dowhuszko, *Senior Member, IEEE*, and Borja Genovés Guzmán, *Member, IEEE*

Abstract—Multi-color Light-Emitting Diode (LED) technology enables a simple approach to increase the throughput of a Visible Light Communications (VLC) system, by using Wavelength-Division Multiplexing (WDM) to transmit independent data streams on different colors. However, to compute the data rate that is achievable in such WDM VLC link, the optical power that leaks between the different colors needs to be estimated accurately, especially when low-cost optical filters are used in reception. So far, the approximations that have been reported in the literature to model the spectral power emission of different color LEDs are not good enough to perform these calculations. Starting from the theoretical spectral emission of a color LED, a closed form expression is derived based on an asymmetric Pearson type VII function, which is shown to approximate accurately the measured spectra of the color LEDs at different working regimes. In addition, the effect that the DC-bias current has on the key parameters of the approximated spectral power emissions, namely the peak and half-maximum wavelengths, as well as the peak spectral emission, are studied. Finally, a new approach is proposed to assess the level of fitness of the derived closed form approximations, using for this purpose the step-size of the MacAdam ellipses that corresponds to the different color LED spectral emissions in the CIE 1931 chromaticity diagram.

Index Terms—Visible Light Communications, Wavelength-Division Multiplexing, Multi-Color LED, Spectral Power Emission, Asymmetric Pearson type VII distribution, Curve fitting, Polynomial approximations, Cross-talk interference, CIE 1931.

I. INTRODUCTION

Visible Light Communication (VLC) has been lately drawing the attention of the research community, and is currently being considered as a technology enabler to satisfy the ever-increasing demand of wireless data traffic, especially in indoor environments [1]. This is because VLC links can support high data rates using low-cost off-the-shelf components, as well as high levels of Physical-layer security. VLC makes use of either a Light-Emitting Diode (LED) or Laser Diode (LD) as transmitter, and a Photodetector (PD) as receiver. In the transmitter side, the data-carrying signal takes the form of an electrical current that drives the intensity of the LED (or LD), which is in charge of the electrical-to-optical conversion. Data rates in the order of few gigabit-per-second (Gbps) have been experimentally demonstrated using both LEDs [2] and LDs [3], [4] as light sources. Though LEDs present a narrower electrical modulation bandwidth (*i.e.*, slower time response) and less directional optical wireless beams when compared to LDs, their simplicity, eye-safety properties, and low cost make them a popular choice

A. A. Dowhuszko is with the Department of Communications and Networking, School of Electrical Engineering, Aalto University, 00076 Aalto, Finland (e-mail: alexis.dowhuszko@aalto.fi).

B. Genovés Guzmán is with the IMDEA Networks Institute, 28918 Leganés, Spain (e-mail: borja.genoves@imdea.org).

for indoor VLC deployments. Therefore, this paper focuses on the use of LEDs as light sources, such that illumination and communication services can be provided simultaneously.

On the receiver side, the time-varying optical power that impinges on the sensitive area of the PD is transformed into an electrical current, from which the data symbols are detected. Thus, the transmission and reception of information in VLC use the Intensity Modulation (IM) with Direct Detection (DD) approach. Moreover, since these optical wireless signals are visible to humans, an equivalent *white* light beam with coordinates near the Planckian locus of the CIE 1931 chromaticity diagram is needed to re-use the light emitted by the multi-color LEDs for illumination. Though Phosphor-Converted (PC)-LED technology is very popular in VLC systems in terms of costs and good Color Rendering Index (CRI), the slow time-response of the yellow phosphor coating limits the data rate that can be achieved. This is the reason why multi-color LEDs emerge as an interesting alternative to address the limitations that PC-LEDs have when used for communications purposes.

Multi-color LEDs have a wider electrical modulation bandwidth than their PC-LED counterparts [5], can implement Wavelength-Division Multiplexing (WDM) to transmit parallel data streams over the same optical wireless link [6], and have the ability to decrease the interference produced by external sources of light and/or adjacent VLC Access Points (APs) in multi-cell scenarios [7], [8], [9]. From a purely analytical perspective, different papers have studied the data rate that tri- and quadri-chromatic white LEDs can achieve under different illumination constraints [10], or the data rate that is feasible with multi-color LEDs when using a Multiple-Input Multiple-Output (MIMO) scheme [11], [12]. However, the use of multi-color LEDs involves further practical challenges that are not usually considered in the literature, such as the cross-talk interference among data streams on different colors, or the variation that the color LED spectral emission experiences as the DC-bias current (or junction/carriers temperature) changes [13].

Most of the papers that study the use of multi-color LEDs for VLC neglect the impact that cross-talk interference between colors have, by claiming that highly-selective (narrow-band) optical filters can be used in the VLC receiver [10], [14], [15]. Unfortunately, such high-quality optical filters are very expensive for massive use and, due to that, not suitable for smart scenarios that rely on a large number of connected sensors and actuators. Low-cost glass or plastic optical filters can be used in these Internet-of-Things (IoT) scenarios, provided that the cross-talk interference that is created between the data streams transmitted on the different colors does not impact the achievable data rate of the VLC link notably. Similarly, other references consider that color

LEDs have an invariant spectral power emission regardless of their working condition, neglecting the effect that the DC-bias current, (heat-sink dependent) junction/carriers temperature, and LED semiconductor parameters have on the optical power that the color LED emits on the different wavelengths [16], [14], [13]. Recently, the variation that the spectral emission of color LEDs experiences has been proposed to implement a new (low-rate) communication channel [17], [18]; however, these studies are purely experimental in nature, and have a lack of an analytical framework that could be used by other researchers to address the different challenges that emerge when using multi-color LEDs to implement a VLC system in practice.

Closed form expressions that model accurately the spectral power emission of color LEDs are needed, and results published in the literature so far are not suitable for designing VLC system using multi-color LEDs. For example, the authors of [13] present a summary of different functions that can be used to model the spectral power emission of color LEDs with different levels of fitness, which include Gaussian, Pearson-VII and piece-wise third-order polynomial (Spline) functions, among others. Similarly, low-order polynomial functions were proposed in [19], split-Gaussian approximation were considered in [20], and merged exponential and Gaussian functions were presented in [21] to model the spectrum of different LED technologies. However, these spectral emission models were studied in these references from a purely empirical perspective, without a mathematical reasoning behind their derivation that justifies the shape of the function that was selected. Moreover, none of these models approximate the tails of the emission spectrum accurately, which is critical to assess correctly the impact of the (inter-color) cross-talk interference, or estimate the Correlated Color Temperature (CCT) and/or CRI of the aggregate white light that the multi-color LED generates [22].

To fill the gap that exists between purely theoretical and purely empirical VLC system designs using the multi-color LED technology, this paper demonstrates that an asymmetric Pearson-VII approximation can be used to model accurately the spectral power emission of color LEDs at different DC-bias currents. Indeed, the proposed asymmetric Pearson-VII model is derived from the theoretical spectral power emission that color LEDs should ideally have, according to the physical mechanisms that govern spontaneous photon emissions. Moreover, the parameters that define the final shape of the asymmetric Pearson-VII approximation are obtained from three representative values that can be easily determined from any measured color LED spectra, namely the peak wavelength (λ_p), the lower half-maximum wavelength ($\lambda_{0.5}^{(1)}$) and the upper half-maximum wavelength ($\lambda_{0.5}^{(2)}$). The effect that the DC-bias current has on the key spectral emission parameters is also studied, and low-order polynomial approximations are derived to estimate these values at different working regimes. Without loss of generality, the same procedure can be utilized to model the effect of other LED parameters that affect its temperature, such as the heat dissipation mechanism, the LED size, thermal rollover, non-linear responses, and transient time characteristics, among others [13]. Finally, the accuracy of the asymmetric Pearson-VII model is validated using the step-size

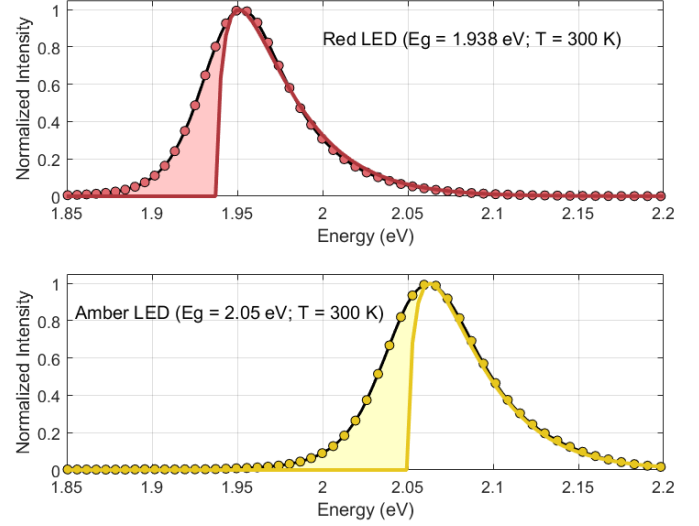


Fig. 1. Measured spectrum (black line with circles) and theoretical spectrum (solid color lines) of two (single) color LEDs as function of the density of energy states E above the band gap energy E_g . Shadowed area below E_g is light emission due to thermal agitation.

of the MacAdam ellipses for the measured and approximated LED spectra in the CIE 1931 chromaticity diagram.

The rest of this paper is organized as follows. Section II presents the theoretical spectral power emission of a color LED based on fundamentals of Physics, whereas Section III derives a closed form approximation based on an asymmetric Pearson-VII function, providing evidence of its accuracy. Section IV studies the effect that the DC-bias current has on the spectral power emission parameters of different color LEDs, evaluating as well the level of fitness that the proposed asymmetric Pearson-VII approximation provides for different working regimes. Finally, conclusions are drawn in Section V.

II. THEORETICAL SPECTRAL POWER EMISSION OF LED

The spontaneous recombination of electron-hole pairs with simultaneous emission of photons is the physical mechanism that models the emission of light in a color LED¹. In theory, the distribution of the photon energy E of a color LED is determined by the product of the density of energy states within the allowed energy band and the Boltzmann energy distribution [23], and is proportional to

$$I_{\text{theo}}(E) \propto \sqrt{E - E_g} \exp\left(-\frac{E}{k_B T_c}\right), \quad (1)$$

where E_g is the gap energy level of the active layer material, k_B is the Boltzmann constant, and T_c is the temperature of the carriers, which is usually higher than the junction temperature.

Fig. 1 shows the spectral power emission of two color LEDs from the LUXEON Rebel color line family when measured

¹Both LEDs and LDs generate radiation via an electrical current that is injected into a P-N junction that generates spontaneous emissions of photons on various wavelengths. However, LDs also have an optical cavity that allows photons on very few wavelength to pass by, which are later on used to stimulate the emission of new photons. This paper focus on the first case, which is suitable to model the spectral emission of color LEDs.

TABLE I
PARAMETERS OF THE MEASURED SPECTRAL EMISSION OF DIFFERENT COLOR LEDs AT TEST CURRENT $I_{dc} = 0.2$ A.

Color	Part No.	E_g (eV)	λ_p (nm)	FWHM (nm)
Red	LXM2-PD01-0040	1.938	635.2	19.3
Red-Orange	LXM2-PH01-0060	1.975	623.2	18.5
Amber	LXML-PL01-0050	2.05	601.1	19.5
Green	LXML-PM01-0090	2.332	529.4	32.6
Green-Blue	LXML-PB01-0070	2.429	507.5	33.1
Blue	LXML-PB01-0023	2.642	467.5	24.1

with the same DC-bias current ($I_{dc} = 200$ mA)². Without loss of generality, the actual spectral power emission for a Red-color LED (LXM2-PD01-0040) and Amber-color LED (LXML-PL01-0050) [24] are presented. According to (1), the peak emission intensity occurs at

$$E_p = E_g + k_B T_c / 2. \quad (2)$$

Table I shows the values of E_g that were computed from the measured emission spectrum of the different color LEDs, including the peak wavelength λ_p and the Full-Width at Half-Maximum (FWHM) of the optical spectrum. To identify the energy levels that correspond to the photons emitted by the given color LED, the well-known Planck-Einstein relation

$$E = \hbar c / \lambda \quad (3)$$

can be used, where \hbar is the Planck's constant, c is the speed of light in vacuum, and λ is the wavelength of the photon. Note that the light emission observed under the active zone gap level (*i.e.*, when $E < E_g$) of Fig. 1 corresponds to thermal agitation of the crystal lattice in the LED chip.

The normalized theoretical emission spectrum of a color LED can be obtained by combining (1) with (2), *i.e.*,

$$\begin{aligned} \tilde{I}_{\text{theo}}(E) &= \frac{I_{\text{theo}}(E)}{I_{\text{theo}}(E_p)} \\ &= \sqrt{\frac{2(E - E_g)}{k_B T_c}} \exp \left\{ -\frac{(E - E_g)}{k_B T_c} + \frac{1}{2} \right\} \\ &= \frac{1}{\left[\left(\frac{k_B T_c}{2(E - E_g)} \right)^{1/4} \exp \left\{ \frac{(E - E_g)}{2k_B T_c} - \frac{1}{4} \right\} \right]^2} = \frac{1}{g^2(E)}. \end{aligned} \quad (4)$$

Let us now focus on the denominator of the normalized emission spectrum, *i.e.*,

$$\begin{aligned} g(E) &= \left(\frac{k_B T_c}{2(E - E_g)} \right)^{1/4} \exp \left\{ \frac{(E - E_g)}{2k_B T_c} - \frac{1}{4} \right\} \\ &= \left(\frac{k_B T_c}{2(E - E_p + k_B T_c / 2)} \right)^{1/4} \exp \left\{ \frac{(E - E_p + k_B T_c / 2)}{2k_B T_c} - \frac{1}{4} \right\}. \end{aligned} \quad (5)$$

²The manufacturer of the color LEDs, *Lumileds*, was selected for pragmatic reasons. Priority was given to the wide palette of the LED colors that was offered, detailed information that was presented in the data sheets, and wide presence of these color LED chips in the market (online retailers). Similar performance results were obtained when using LED chips from other different manufacturers, as the effects that are modeled in this paper depend mainly on the semiconductor materials that are used to build the color LEDs [13].

Then, replacing the photon energy with the corresponding wavelength-dependent relation in (3), we have that

$$\begin{aligned} g(\lambda) &= \left(\frac{(k_B T_c) / (\hbar c)}{(2/\lambda - 2/\lambda_p) + (k_B T_c) / (\hbar c)} \right)^{1/4} \\ &\times \exp \left\{ \frac{1/\lambda - 1/\lambda_p + (k_B T_c) / (2\hbar c)}{2(k_B T_c) / (\hbar c)} - \frac{1}{4} \right\} \\ &\approx g(\lambda_p) + g'(\lambda_p)(\lambda - \lambda_p) + \frac{1}{2}g''(\lambda_p)(\lambda - \lambda_p)^2, \end{aligned} \quad (6)$$

where the latter expression corresponds to the second-order Taylor series expansion of $g(\lambda)$ centered around λ_p . Note that since the global maximum of the normalized spectral emission $\tilde{I}_{\text{theo}}(\lambda)$ takes place at λ_p , it is possible to show that $g(\lambda_p) = 1$ and $g'(\lambda_p) = 0$. Due to that, we have that

$$g(\lambda) \approx 1 + \frac{(\lambda - \lambda_p)^2}{(\sqrt{2}\lambda_p^2/a_1)^2}, \quad a_1 = \frac{\hbar c}{k_B T_c}. \quad (7)$$

Finally, after replacing (7) into (4), we obtain a spectral power emission that resembles the well-known Pearson-VII probability density function, *i.e.*,

$$\tilde{I}_{\text{theo}}(\lambda) \approx \frac{A}{\left(1 + \frac{(\lambda - C)^2}{W} \right)^S}, \quad (8)$$

where $A = 1$, $C = \lambda_p$, $W = 2\lambda_p^4/a_1^2$, and $S = 2$.

Based on this theoretical derivation, we are now ready to show an accurate curve fitting model based on the Pearson-VII function. This distribution has been used in the past to approximate the stochastic behavior of peak radiation on different parts of the electromagnetic spectrum, such as on the X-ray region [25]. However, instead of approximating the mode (C), scale parameter (W) and shape parameter (S) of the Pearson-VII function using Least Mean Square (LMS) estimation, this paper derives the formulas to compute them in closed form. These formulas depend on the peak and half-maximum wavelengths of the color LED spectrum.

We note that in actual (measured) color LED spectral emissions, the Boltzmann exponential behavior that (1) predicts on the right-hand side of the distribution can be easily recognized. However, the sharp spectrum cut-off that the theory predicts on the low energy side of the peak wavelength is not observed. This behavior, which is attributed to thermal agitation of the crystal lattice of the diode [26], has also an exponential behavior that can be modeled accurately selecting the proper shaping parameter of the Pearson-VII formula on that side. This is the reason why an asymmetric (piece-wise) Pearson-VII function is now introduced, to estimate with good accuracy the spectral power distribution on both left- and right-hand side parts.

III. CLOSED FORM APPROXIMATION OF THE SPECTRAL POWER EMISSION OF A COLOR LED

The optical spectrum emitted by a color LED depends on its carriers (or junction) temperature which, at the same time, is strongly dependent on the DC-bias current that is used

to polarize it³. An initial closed form approximation of the normalized spectral power emission of a color LED can be based on the Gaussian function [27] but, unfortunately, this simplistic model does not take into account the asymmetric shape of the distribution that is predicted by the theory of spontaneous photon emission in LEDs [13] (see Section II), and that practical measurements corroborates in references such as [28] (see Section III-B). The theoretical emission spectrum of a color semiconductor LED has a square root form in the left-hand side due to the joint density of states, while the right-hand side has an exponential form, which depends on the distribution of carriers in the allowed bands and follows a Boltzmann distribution [23]. Moreover, there are other phenomena, such as the thermal agitation of crystal lattice in the LED that generates emission of photons under the active zone gap level (*i.e.*, for energy levels $E < E_g$), which introduce additional differences between the empirical and theoretical spectral power emissions [26]. The stochastic modelling of these phenomena is not straightforward, and the identification of distributions that can be used to derive formulas to assess the performance of multi-color LED systems are desirable.

One option to address this property is to split the spectral power emission function of the LED into two parts: one to the left-hand side of the peak wavelength and the other one to the right-hand side of it [29]. Since the tail of a Gaussian distribution is not *heavy* enough to model accurately the LED emission far away from the peak wavelength, we use the approximation presented in (8) as reference, which was derived from the theoretical (ideal) spectral power emission that a color LED should have according to the principles of Physics.

A. Parameters of the asymmetric Pearson-VII approximation

Let us assume that from each measured spectral power emission of an LED with color index c , we are able to determine the peak wavelength $\lambda_{p,c}$ and the extreme wavelengths that define the width of the optical emission at half-maximum. That is, we consider that it is possible to measure the left- and right-side half-maximum wavelengths $\lambda_{0.5,c}^{(1)}$ and $\lambda_{0.5,c}^{(2)}$, such that $\text{FWHM}_c = \lambda_{0.5,c}^{(2)} - \lambda_{0.5,c}^{(1)}$ for the LED with color index c .

Then, the aim is to determine the value of W such that

$$\tilde{I}(\lambda_{0.5}) \approx \left(1 + \frac{(\lambda_{0.5} - \lambda_p)^2}{W} \right)^{-S} = 0.5 \quad (9)$$

is verified, which can be computed from

$$W = \frac{(\lambda_{0.5} - \lambda_p)^2}{2^{1/S} - 1}. \quad (10)$$

Then, W can be computed for the left- or right-side part of the LED spectral power emission, by just replacing the half-maximum wavelength $\lambda_{0.5}^{(1)}$ or $\lambda_{0.5}^{(2)}$ in (10), respectively.

³There are other parameters that affect the relation between the DC-bias current and temperature in an LED, such as the heat-sink that is used for thermal dissipation, the LED chip size and case package, among others. Without loss of generality, this paper focuses on the effect that the DC-bias current has on the spectral power emission of color LEDs, as it represents a parameter that can be easily controlled to obtain thermally stable situations.

TABLE II
PARAMETERS OF THE APPROXIMATED SPECTRAL POWER EMISSION OF COLOR LEDs AT TEST CURRENT $I_{dc} = 0.2$ A.

Color	Symb.	λ_p (nm)	$\lambda_{0.5}^{(1)}$ (nm)	$\lambda_{0.5}^{(2)}$ (nm)	W_c (nm ²)	m_c
Red	'r'	635.2	624.5	643.8	333.65	0.1716
Red-Orange	'ro'	623.2	613.1	631.6	309.60	0.2045
Amber	'a'	601.1	590.7	610.2	349.39	0.2526
Green	'g'	529.4	514.6	547.2	961.30	-0.2043
Green-Blue	'gb'	507.5	492.1	525.2	1004.90	-0.2473
Blue	'b'	467.5	455.8	479.9	547.35	-0.3218

Since it is more practical to find a unique closed form formula that is valid to approximate the measured spectral emission a color LED in the whole range of visible light wavelengths, we propose to use the equivalent expression

$$\tilde{I}_c(\lambda) = \left(1 + \frac{(\lambda - \lambda_{p,c})^2}{W_c [1 + m_c \text{sign}(\lambda - \lambda_{p,c})]} \right)^{-S_c(\lambda)}, \quad (11)$$

where

$$W_c = \frac{W_c^{(2)} + W_c^{(1)}}{2}, \quad m_c = \frac{W_c^{(2)} - W_c^{(1)}}{W_c^{(2)} + W_c^{(1)}}, \quad (12)$$

define the width and the asymmetric coefficient of the spectral power emission, respectively, with

$$W_c^{(2)} = \frac{(\lambda_{0.5,c}^{(2)} - \lambda_{p,c})^2}{2^{1/S_c(\lambda_{0.5,c}^{(2)})} - 1}, \quad W_c^{(1)} = \frac{(\lambda_{0.5,c}^{(1)} - \lambda_{p,c})^2}{2^{1/S_c(\lambda_{0.5,c}^{(1)})} - 1}. \quad (13)$$

We note that, in order to fit the measured data with the asymmetric spectral emission approximation based on the Pearson-VII distribution, the shape parameter is given by

$$S_c(\lambda) = 3 - \text{sign}(\lambda_{p,c} - \lambda), \quad c \in \{\text{r, ro, a}\} \quad (14)$$

when the LED color is Red (r), Red-Orange (ro), and Amber (a), whereas

$$S_c(\lambda) = 3 - \text{sign}(\lambda - \lambda_{p,c}), \quad c \in \{\text{g, gb, b}\} \quad (15)$$

when the LED color is Green (g), Green-Blue (gb), and Blue (b), respectively. Therefore, the *heavy* tail of the spectral power emission for the color LED that concentrates most of the emission probability density has a shape parameter $S_c = 2$, whereas the *light* tail that concentrates a lower emission probability density has a shape parameter $S_c = 4$

B. Fitness of the derived approximation for the spectral power emission of color LEDs

The parameters that characterize the closed form formula (11), which are used to approximate the spectral power emission of the different color LEDs under study, are summarized in Table II. The accuracy of these approximations, when compared to actual measurements when the DC-bias current was set to $I_{dc} = 200$ mA, are shown in Fig. 2. Based on the results reported in this figure, it is possible to conclude that the proposed approximation, based on an asymmetric Pearson-VII function, fits very well the actual measured spectral power emission of the different color LEDs under analysis.

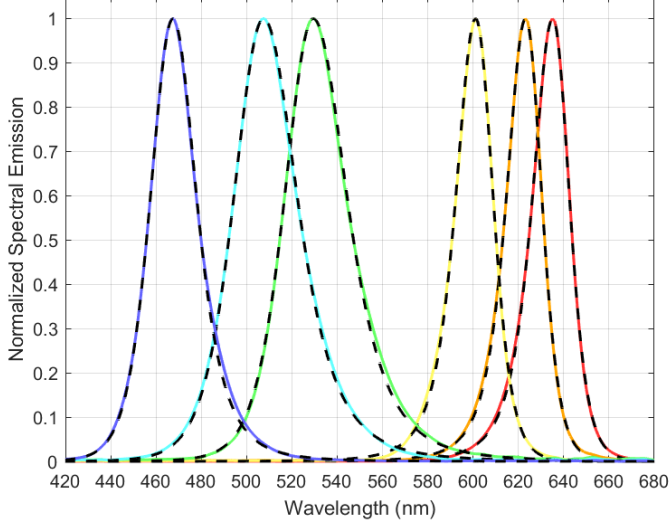


Fig. 2. Measured spectrum (color lines) and closed form approximation based on asymmetric Pearson-VII (dashed-lines) when the DC-bias current is 200 mA. Spectral emissions from left to right: Blue, Green-Blue, Green, Amber, Red-Orange, and Red color LEDs.

As expected, the Green, Green-Blue (Cyan), and Blue LEDs are the ones with widest spectral emission (*i.e.*, largest FWHM parameter). On the other hand we have the Red-Orange, Red, and Amber LEDs, which have an spectral power emission that is more concentrated around the corresponding peak wavelength. It is interesting to note that the asymmetric coefficient m_c is positive for the Red, Red-Orange, and Amber LEDs, and negative for the Green, Green-Blue, and Blue LEDs. Due to that, we have that the probability density of the spectral power emission of the former group of LEDs (*i.e.*, Red, Red-Orange, and Amber) is concentrated on wavelengths that are below the peak wavelength $\lambda_{p,c}$. The opposite situation takes place with the second group of color LEDs (*i.e.*, Green, Green-Blue, and Blue), where most of the power emission takes place on wavelengths λ that are above the peak wavelength $\lambda_{p,c}$.

IV. EXPERIMENTAL RESULTS

This section studies the effect that the DC-bias current has on the parameters of the asymmetric Pearson-VII function that is used to approximate the actual spectral power emission of the color LEDs listed in Table I. For practical reasons, the derived Pearson-VII approximation was validated using six color LED models from the LUXEON Rebel color line family. Nevertheless, the same approach can be applied to other LED manufacturers, models and colors, as the principles of Physics that model the spectral power emission of these color LEDs are the same, and depend mainly on the semiconductor material that is used to generate the visible light beam. After that, the fitness of these approximations is compared with the actual measured spectral emissions at different DC-bias currents.

A. Parameters of the spectral emission versus DC-bias current

Polynomial approximations are used in this paper to estimate the effect of the DC-bias current has on the different

TABLE III
COEFFICIENTS OF MMSE POLYNOMIAL APPROXIMATION OF PEAK WAVELENGTH, LEFT-SIDE AND RIGHT-SIDE HALF-MAXIMUM WAVELENGTH FOR DIFFERENT COLOR LEDs.

Color	Peak wavelength		Left half-maximum		Right half-maximum	
	$\hat{\lambda}_{p,c} = a_{p,c}I_{dc} + b_{p,c}$	$\hat{\lambda}_{0.5,c}^{(1)} = a_{0.5,c}^{(1)}I_{dc} + b_{0.5,c}^{(1)}$	$a_{0.5,c}^{(1)}$	$b_{0.5,c}^{(1)}$	$a_{0.5,c}^{(2)}$	$b_{0.5,c}^{(2)}$
'r'	0.0229	630.5	0.0178	621.0	0.0275	638.5
'ro'	0.0127	620.5	0.0082	611.4	0.0137	628.8
'a'	0.0364	593.4	0.0298	584.2	0.0406	601.5
'g'	-0.0185	532.8	-0.0150	517.5	-0.0205	550.8
'gb'	-0.0233	511.5	-0.0371	498.9	-0.0139	527.4
'b'	0.0024	467.1	-0.0037	456.6	0.0077	478.6

TABLE IV
COEFFICIENTS OF MMSE POLYNOMIAL APPROXIMATION OF PEAK SPECTRAL EMISSION FOR DIFFERENT COLOR LEDs.

Color	Peak spectral emission		
	$\hat{A}_{m,c} = a_{m,c}I_{dc}^2 + b_{m,c}I_{dc} + c_{m,c}$	$a_{m,c}$	$b_{m,c}$
'r'	-1.0161	1.2744	-1.1659×10^{-3}
'ro'	-0.6640	1.3923	-3.2623×10^{-3}
'a'	-1.8419	0.6064	-0.5964×10^{-3}
'g'	0.0194	0.0822	-0.2943×10^{-3}
'gb'	-1.3963	1.0573	0.0641×10^{-3}
'b'	-2.5067	2.3526	8.7045×10^{-3}

parameters that characterize the spectral power emission of a color LED. Without loss of generality, the Minimum Mean Square Error (MMSE) criterion is used to estimate the parameters of the polynomial function, in which the peak wavelength

$$\hat{\lambda}_{p,c} = a_{p,c}I_{dc} + b_{p,c} \quad (16)$$

and the left- and right-side half-maximum wavelengths

$$\hat{\lambda}_{0.5,c}^{(1)} = a_{0.5,c}^{(1)}I_{dc} + b_{0.5,c}^{(1)}, \quad \hat{\lambda}_{0.5,c}^{(2)} = a_{0.5,c}^{(2)}I_{dc} + b_{0.5,c}^{(2)}, \quad (17)$$

respectively, are approximated with first-order polynomials. The coefficients that were computed are given in Table III.

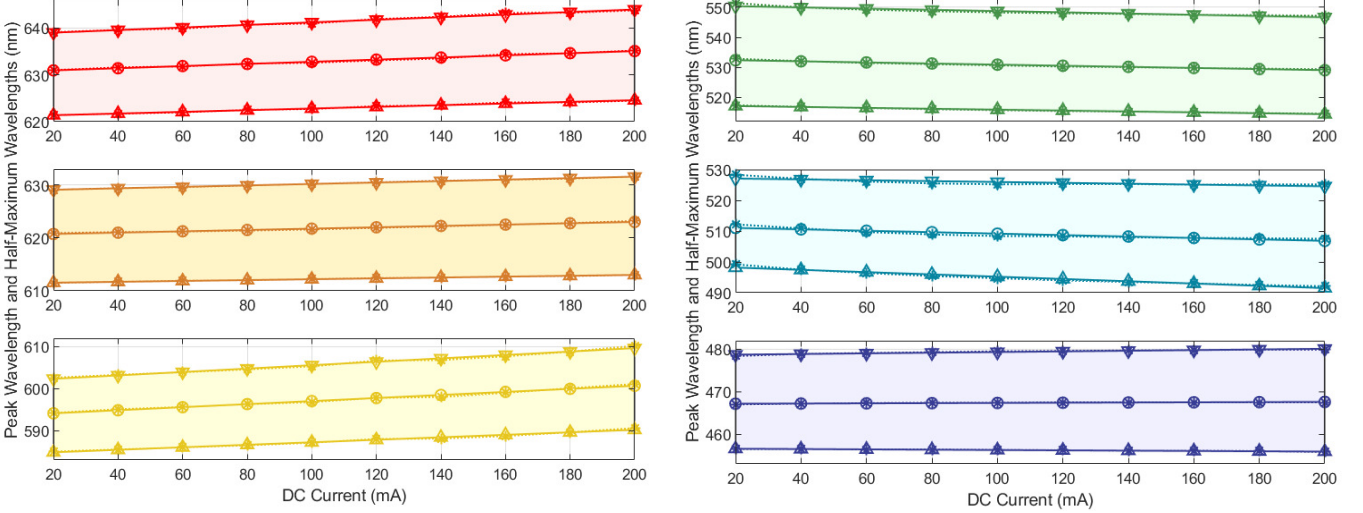
Similarly, the peak spectral emission that corresponds to the different DC-bias currents for the color LEDs under study can be approximated as a second-order polynomial, *i.e.*,

$$\hat{A}_{m,c} = a_{m,c}I_{dc}^2 + b_{m,c}I_{dc} + c_{m,c}, \quad (18)$$

where the values of the computed polynomial coefficients are shown in Table IV. We note that the peak spectral emissions were measured when the Illuminance Spectrophotometer [30] was placed at a one-meter distance from the LED in its boresight direction (*i.e.*, in the axis of the maximum radiated power). Therefore, when the objective is to determine the shape of the spectral emission at different DC-bias currents, the area of the asymmetric Pearson-VII function can be scaled accordingly, to obtain the target total optical emission, which is given by $P_{o,c} \approx A_{m,c} \int_{\lambda_{min}}^{\lambda_{max}} \tilde{I}_c(\lambda)d\lambda$.

Fig. 3 shows the effect that the DC-bias current has on the peak wavelength $\lambda_{p,c}$ and the Full-Width Half-Maximum

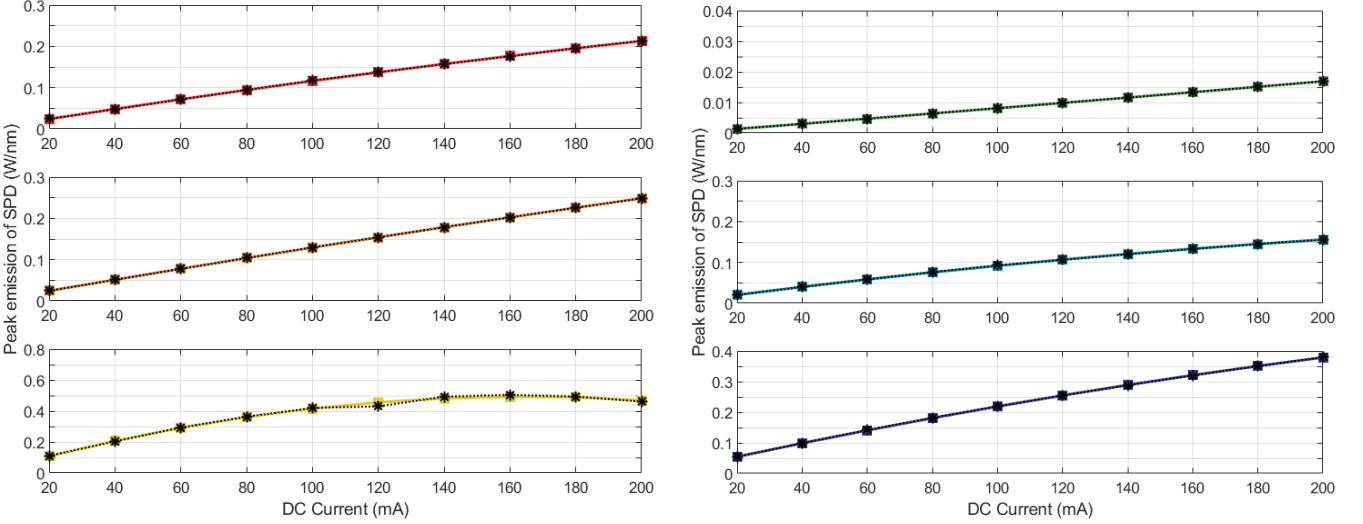
$$\text{FWHM} = \lambda_{0.5,c}^{(2)} - \lambda_{0.5,c}^{(1)}, \quad (19)$$



(a) Red (upper-panel), Orange (middle-panel) and Amber (lower-panel).

(b) Green (upper-panel), Cyan (middle-panel) and Blue (lower-panel).

Fig. 3. Closed form approximation of the peak wavelength (circles), as well as for the left-side (upper-pointing triangles) and right-side (lower-pointing triangles) half-maximum wavelengths for the six color LEDs under evaluation. Point values (**) were measured.



(a) Red (upper-panel), Orange (middle-panel) and Amber (lower-panel).

(b) Green (upper-panel), Cyan (middle-panel) and Blue (lower-panel).

Fig. 4. Closed form second-order polynomial approximation of the peak spectral emission that was measured for the six color LEDs under evaluation (squares). Point values (**) were measured.

bandwidth of the different color LEDs under evaluation. As general trend, the FWHM parameter increased as the DC-bias current grew for the color LEDs under study. In addition, for the Red, Red-Orange, and Amber LEDs, the peak and half-maximum wavelengths increased as function of the DC-bias current, whereas the opposite situation took place for the Green, Green-Blue (Cyan), and Blue LEDs. The LED that showed the most stable spectral emission parameters was the Blue LED, followed by the Red-Orange and Green LEDs. On the other hand, the spectral emission that was most influenced by the DC-bias current was the one that corresponded to the Amber LED, followed by the Green-Blue (Cyan) and Red LEDs. It was also shown that the effect of the DC-bias current on the peak and half-maximum wavelengths can be accurately modeled with a first-order polynomial approximation.

Similarly, Fig. 4 shows the effect that the DC-bias current (I_{dc}) has on the peak spectral emission ($A_{m,c}$) of the six color LEDs under evaluation. From these plots, it is possible to corroborate that those color LEDs that concentrate their power emission in the extremes of the visible light spectrum (*i.e.*, Red, Red-Orange, Blue-Green and Blue) have a higher radiant flux efficacy, measured as the relation between the radiant optical energy emitted versus the input electrical energy, than those LEDs whose emission is concentrated in the central part of the visible light band (*i.e.*, Amber and Green). More precisely, the peak spectral emission for the Amber and Green LEDs was an order of magnitude smaller than the one that corresponded to the other color LEDs (see Fig. 4).

The radiant flux efficacy is a very relevant parameter when designing a VLC system using multi-color LED, as most of

the data sheets only show information about the luminous efficacy of the LED. Note that the luminous efficacy, measured in radiant luminous emission versus input optical power [24], is a relevant parameter for illumination purposes, as it takes into account the sensitivity of the human eye to the radiation on different portions of the visible light spectrum. Then, such a figure of merit is not a relevant parameter for a VLC system design, as spectral responsivity of a photodetector has a different shape when compared to the one that corresponds to the human eye. For example, a black silicon photodetector [31], [32] has its maximum (minimum) responsivity, measured in Ampere/Watt, in the Red (Blue) light regions of the visible light band. In contrast, the human eye has its peak sensitivity in the Green light region and the minimum sensitivity in the Red and Blue light regions, respectively. Finally, based on the plots shown in Fig. 4, it is possible to validate empirically that the effect that the DC-bias current has on the peak spectral emission of the color LEDs under study can be accurately estimated using second-order polynomial approximations.

B. Fitness of proposed asymmetric Person-VII approximation

Figure 5 shows the goodness of the proposed asymmetric Pearson-VII approximation, which was used to model accurately the actual spectral power emission of the six color LEDs under study at different polarization (DC-bias) points. Without loss of generality, three DC-current are included in these plots to facilitate the visibility of results, namely 60 mA, 100 mA, and 200 mA. As expected, there are no major differences between the closed form approximations and the measured spectral power emissions for the six color LEDs under study in the whole range of wavelengths that correspond to the visible light band. Based on this, it is possible to conclude that not only the asymmetric Pearson-VII approximation proposed in Section III-A provides a good level of fitness, but also that the parameters of these distributions (*i.e.*, peak wavelength, left- and half-side half-maximum wavelengths, and peak spectral emission) can be accurately estimated using low-order polynomial approximations, whose coefficients can be computed using MMSE interpolation as described in Section IV-A.

In order to assess the goodness of the proposed asymmetric Pearson-VII approximation in an objective way, this paper uses two systematic approaches. The first approach is based on the Euclidean Distances between the coordinates of the estimated and the measured spectral power emission in the CIE 1931 chromaticity diagram. The second approach uses the step-size of the MacAdam ellipse, centered in the measured spectral power emission coordinate, that contains the estimated coordinate in the CIE 1931 chromaticity diagram.

In the first approach, the coordinates that corresponds to the measured spectral emission, (x_c, y_c) , and the approximated closed form expression, $(\tilde{x}_c, \tilde{y}_c)$, are determined in the CIE 1931 chromaticity diagram for the six color LEDs under study (see Table V). Then, the Euclidean distance between measured and approximated spectral emissions, *i.e.*,

$$\|(\Delta x_c, \Delta y_c)\| = \sqrt{(\tilde{x}_c - x_c)^2 + (\tilde{y}_c - y_c)^2}, \quad (20)$$

is used as a first metric of the accuracy that the proposed asymmetric Pearson-VII approximation provides. Based on

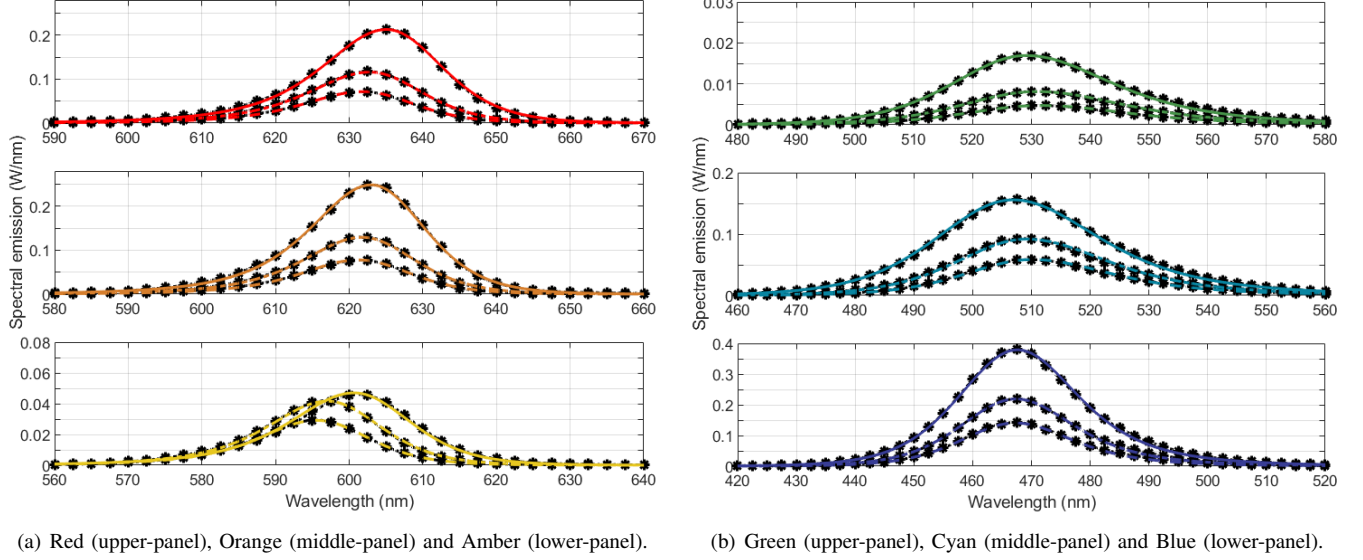
TABLE V
EUCLIDEAN DISTANCE $(\Delta x_c, \Delta y_c)$ AND STEP FOR THE MACADAM ELLIPSE CENTERED ON (x_c, y_c) THAT CONTAINS THE COORDINATES $(\tilde{x}_c, \tilde{y}_c)$ AT DIFFERENT DC-BIAS CURRENTS.

Color	I_{dc} (mA)	CIE 1931 Measured (x_c, y_c)	CIE 1931 Approximated $(\tilde{x}_c, \tilde{y}_c)$	Step of MacAdam ellipse	Euclidean Distance $\ (\Delta x, \Delta y)\ $
'r'	60	(0.6904, 0.3032)	(0.6952, 0.3043)	1.90	0.0049
'r'	100	(0.6921, 0.3027)	(0.6960, 0.3035)	1.55	0.0040
'r'	200	(0.6986, 0.2995)	(0.6978, 0.3016)	1.30	0.0022
'ro'	60	(0.6702, 0.3221)	(0.6778, 0.3217)	3.20	0.0076
'ro'	100	(0.6728, 0.3213)	(0.6782, 0.3212)	2.20	0.0054
'ro'	200	(0.6720, 0.3187)	(0.6793, 0.3201)	2.90	0.0074
'a'	60	(0.5852, 0.4084)	(0.5871, 0.4118)	1.30	0.0039
'a'	100	(0.5924, 0.4030)	(0.5933, 0.4055)	1.05	0.0027
'a'	200	(0.6093, 0.3861)	(0.6078, 0.3910)	2.90	0.0051
'g'	60	(0.2382, 0.7069)	(0.2319, 0.7209)	2.90	0.0154
'g'	100	(0.2308, 0.7156)	(0.2273, 0.7233)	1.60	0.0085
'g'	200	(0.2230, 0.7182)	(0.2157, 0.7288)	2.70	0.0129
'gb'	60	(0.1053, 0.6745)	(0.1063, 0.6796)	0.95	0.0052
'gb'	100	(0.1004, 0.6563)	(0.1048, 0.6629)	2.05	0.0079
'gb'	200	(0.1019, 0.6196)	(0.1024, 0.6170)	0.50	0.0026
'b'	60	(0.1287, 0.0705)	(0.1293, 0.0685)	1.50	0.0021
'b'	100	(0.1289, 0.0715)	(0.1293, 0.0694)	1.50	0.0021
'b'	200	(0.1296, 0.0721)	(0.1291, 0.0716)	1.05	0.0007

these results, it was possible to conclude that the derived approximations worked very well, specially for the Blue, Red and Amber LED spectral power emissions. Performance was slightly degraded for the Green-Blue (Cyan), Red-Orange, and Green LED spectral emissions, but in most of these cases the Euclidean distance $\|(\Delta x_c, \Delta y_c)\|$ was in the order of 0.01.

The study of the Euclidean distance between the CIE 1931 coordinates that corresponds to the actual (measured) and approximated (estimated) spectral power emissions may not be considered as a fair figure of merit, as same distances in the CIE 1931 diagram do not necessarily mean that the variability of the chromaticity will have the same effect on the human eye. Therefore, the quality of the fitness would not only depend on the Euclidean distance, but also on the portion of the visible light band (*i.e.*, colors) in which the LED concentrates most of its emitted optical power. For example, the MacAdam ellipses drawn with the same step size, with center points located at different positions in the CIE 1931 chromaticity diagram, do not have the same size, rotation angle, and shape. Actually, the Euclidean distance could be considered as relevant figure of merit for those light sources whose coordinates are close to the Planckian locus, provided that the chromaticity coordinates (u', v') in the CIE 1976 diagram are used instead. However, some minor variations are still present in this situation, which may change slightly the radii and shapes of the ellipses [33].

In order to address this limitation, a novel approach is proposed based on the n -step metric, where the figure of merit is equal to the step-size of the MacAdam ellipse with center in the coordinates (x_c, y_c) of the measured spectrum, such that the scaled ellipse encompasses the coordinates $(\tilde{x}_c, \tilde{y}_c)$ that corresponds to the approximated spectrum. Fig. 6 plots the CIE 1931 chromaticity diagram with the coordinates that corresponds to the measured and approximated spectral



(a) Red (upper-panel), Orange (middle-panel) and Amber (lower-panel).

(b) Green (upper-panel), Cyan (middle-panel) and Blue (lower-panel).

Fig. 5. Fitness of the proposed asymmetric Pearson-VII approximation for the six color LEDs under study when estimating the peak wavelength, half-maximum wavelengths, and peak spectral emission with closed form polynomial formulas at $I_{dc} = 60$ mA, 100 mA, and 200 mA. Point values (*) were measured.

emissions, as well as the minimum n -step MacAdam ellipses. The MacAdam ellipses for the six LEDs under study were computed with the aid of the *LED Color Calculator tool* provided by OSRAM [34], which employs the derivations presented in [35] and [36] for computing the MacAdam ellipses, interpolated from the original 25 ellipses identified by MacAdam in [37]. The resulting step is also included in Table V for the six color LEDs under study at different DC-bias currents. Note that in all these cases, the step size n for the different colors and DC-bias currents under study was always lower than 3. Then, taking into account that ANSI set as tolerance the 4-step MacAdam ellipse, we conclude that the proposed asymmetric Pearson-VII approximation complies with the contemporary chromaticity standards, and represents an excellent closed form approach for modelling the spectral emission of color LEDs not only around the peak wavelength, but also in the lower (left-side) and upper (right-side) tails.

V. CONCLUSION

The derivation of closed form expressions that approximate accurately the measured spectral power emissions of color LEDs at different DC-bias currents is necessary to assess the data rate performance of a VLC system using multi-color LEDs. Starting from the theoretical spectral power emission that a color LED should have, an asymmetric Pearson-VII approximation was obtained using as fitting parameters the peak wavelength, half-maximum wavelengths, and peak spectral emissions. In addition, the effect that the DC-bias current has on the parameters that define the approximated spectral power emission was also modeled using a first-order polynomial function for the peak and half-maximum wavelengths, and a second-order polynomial function for the peak spectral emission. Finally, a new approach was presented to assess the goodness of the derived approximation, in which the n -step size of the MacAdam ellipse was used as fitness

indicator. Six different commercial color LEDs were evaluated at different DC-bias currents, and the accuracy of the proposed asymmetric Pearson-VII approximation was shown to work very well. Thanks to this model, the cross-talk interference in a WDM optical wireless link using multi-color LEDs in transmission and low-cost optical filters in reception can be estimated, predicting with good accuracy the achievable data rate using different combinations of LED colors. A comprehensive study of the VLC link performance can now be carried out for different working regimes, with the possibility to design the multi-color VLC receiver accordingly, using suitable optical filters that provide the best trade-off between achievable data rate per color (due to the inter-color power leakage) and the implementation cost of the optical filters (due to the optical passband selectivity). Moreover, the illuminance (LX) and chromaticity (CCT and CRI) of the aggregate white light that the multi-color LED generates can be accurately estimated, such that it can verify illumination requirements.

ACKNOWLEDGMENT

This publication has been based upon work from COST Action CA19111 NEWFOCUS, supported by COST (European Cooperation in Science and Technology). Besides, this work has been partially funded by Juan de la Cierva Formación grant (FJC2019-039541-I / AEI / 10.13039/501100011033), granted to the author B. Genovés Guzmán.

REFERENCES

- [1] L. Hanzo, H. Haas, S. Imre, D. O'Brien, M. Rupp, and L. Gyongyosi, "Wireless myths, realities, and futures: from 3G/4G to optical and quantum wireless," *Proc. IEEE*, vol. 100, no. Special Centennial Issue, pp. 1853–1888, May 2012.
- [2] S. Rajbhandari *et al.*, "A multigigabit per second integrated multiple-input multiple-output VLC demonstrator," *J. Lightw. Technol.*, vol. 35, no. 20, pp. 4358–4365, Oct. 2017.
- [3] B. Janjua *et al.*, "Going beyond 4 Gbps data rate by employing RGB laser diodes for visible light communication," *Opt. Express*, vol. 23, no. 14, pp. 18 746–18 753, July 2015.

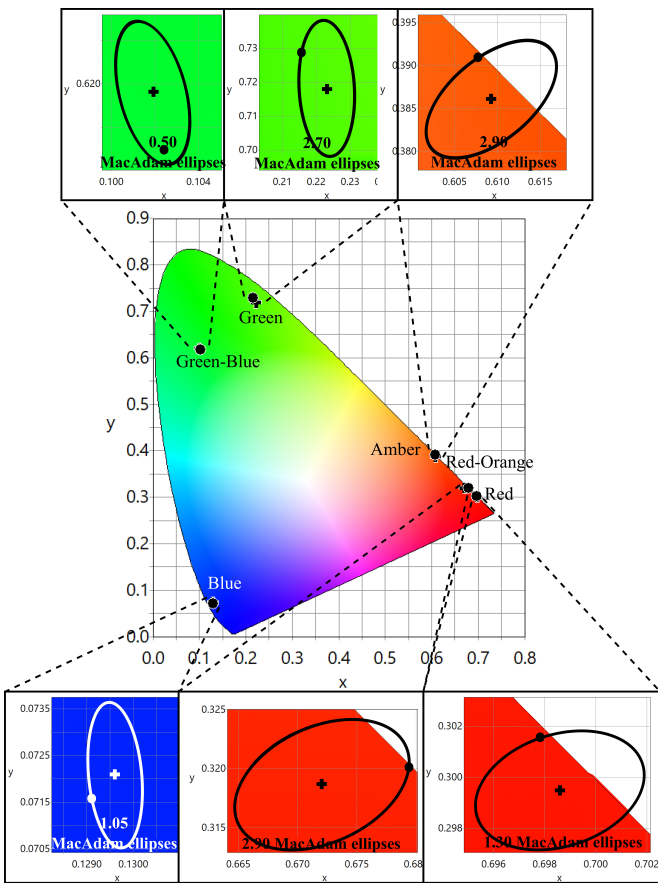


Fig. 6. CIE 1931 chromaticity diagram with measured (crosses) and approximated coordinates (circles) when DC-bias current is set to $I_{dc} = 200$ mA. The MacAdam ellipses with center at the measured points have a step-size such that it includes the approximated points.

- [4] T.-C. Wu, Y.-C. Chi, H.-Y. Wang, C.-T. Tsai, Y.-F. Huang, and G.-R. Lin, "Tricolor R/G/B laser diode based eye-safe white lighting communication beyond 8 Gbit/s," *Scientific Reports*, vol. 7, no. 11, pp. 1–10, Jan. 2017.
- [5] Y. Wang, L. Tao, X. Huang, J. Shi, and N. Chi, "8-Gb/s RGBY LED-based WDM VLC system employing high-order CAP modulation and hybrid post equalizer," *IEEE Photon. J.*, vol. 7, no. 6, pp. 1–7, Dec. 2015.
- [6] H. Chun *et al.*, "LED based wavelength division multiplexed 10 Gb/s visible light communications," *J. Lightw. Technol.*, vol. 34, no. 13, pp. 3047–3052, July 2016.
- [7] A. Dowhuszko and A. I. Pérez-Neira, "Achievable data rate of coordinated multi-point transmission for visible light communications," in *Proc. IEEE Int. Symp. Personal, Indoor, and Mobile Radio Commun.*, Oct. 2017, pp. 1–7.
- [8] B. Genovés Guzmán, A. Dowhuszko, V. Gil Jiménez, and A. Pérez-Neira, "Cooperative transmission scheme to address random orientation and blockage events in VLC systems," in *Proc. Int. Symp. Wireless Commun. Syst.*, Aug. 2019, pp. 351–355.
- [9] B. Genovés Guzmán, A. Dowhuszko, V. Gil Jiménez, and A. Pérez-Neira, "Resource allocation for cooperative transmission in optical wireless cellular networks with illumination requirements," *IEEE Trans. Commun.*, vol. 68, no. 10, pp. 6440–6455, July 2020.
- [10] D. Karunatilaka, V. Kalavally, and R. Parthiban, "Improving lighting quality and capacity of OFDM-based WDM-VLC systems," *IEEE Photon. Tech. Lett.*, vol. 28, no. 20, pp. 2149–2152, Oct. 2016.
- [11] R. Wang, Q. Gao, J. You, E. Liu, P. Wang, Z. Xu, and Y. Hua, "Linear transceiver designs for MIMO indoor visible light communications under lighting constraints," *IEEE Trans. Commun.*, vol. 65, no. 6, pp. 2494–2508, June 2017.
- [12] J. Dong, Y. Zhang, and Y. Zhu, "Convex relaxation for illumination control of multi-color multiple-input-multiple-output visible light communications with linear minimum mean square error detection," *Appl. Opt.*, vol. 56, no. 23, pp. 6587–6595, Aug. 2017.
- [13] T. Khanh, P. Bodrogi, Q. Vinh, and H. Winkler, *LED Lighting: Technology and Perception*. Wiley, Dec. 2014.
- [14] C. Gong, S. Li, Q. Gao, and Z. Xu, "Power and rate optimization for visible light communication system with lighting constraints," *IEEE Trans. Signal Process.*, vol. 63, no. 16, pp. 4245–4256, June 2015.
- [15] R. Jiang, Z. Wang, Q. Wang, and L. Dai, "Multi-user sum-rate optimization for visible light communications with lighting constraints," *J. Lightw. Tech.*, vol. 34, no. 16, pp. 3943–3952, June 2016.
- [16] Y. Zuo and J. Zhang, "Energy-efficient optimization design for the multi-color LED based visible light communication systems under illumination constraints," *Appl. Sci.*, vol. 9, no. 1, pp. 1–14, Dec. 2018.
- [17] D. Moreno, J. Rufo, V. Guerra, J. Rabada, and R. Perez-Jimenez, "Effect of temperature on channel compensation in optical camera communication," *Electronics*, vol. 10, no. 3, pp. 1–20, Jan. 2021.
- [18] —, "Optical multispectral camera communications using led spectral emission variations," *IEEE Photon. Tech. Lett.*, vol. 33, no. 12, pp. 591–594, May 2021.
- [19] P. Dupuis, E. Purwanto, N. Sinisuka, and G. Zissis, "LED spectrum optimal modelization," in *Proc. IEEE Industry Applications Society Annual Meeting*, Sept. 2018, pp. 1–12.
- [20] H. Jin, S. Jin, K. Yuan, and S. Cen, "Two-part Gauss simulation of phosphor-coated LED," *IEEE Photon. J.*, vol. 5, no. 4, pp. 1–10, Aug. 2013.
- [21] M. Raypah, M. Devarajan, and F. Sulaiman, "Modeling spectra of low-power SMD LEDs as a function of ambient temperature," *IEEE Trans. Electron Devices*, vol. 64, no. 3, pp. 1180–1186, Mar. 2017.
- [22] A. Dowhuszko, M. Ilter, P. Pinho, R. Wichman, and J. Hämäläinen, "Effect of the color temperature of LED lighting on the sensing ability of visible light communications," in *Proc. IEEE Int. Conf. Commun. Workshops*, June 2021, pp. 1–6.
- [23] E. Schubert, *Light-Emitting Diodes*, 2nd ed. Cambridge University Press, 2006.
- [24] Lumileds, "LUXEON Rebel color line — High flux and efficacy on industry's most widely used color LED platform," Nov. 2017.
- [25] M. Hall, V. Veeraraghavan, H. Rubin, and P. Winchell, "The approximation of symmetric X-ray peaks by Pearson type VII distributions," *Journal of Applied Crystallography*, vol. 10, no. 1, pp. 66–68, Feb. 1977.
- [26] Y. Deshayes, L. Bechou, F. Verdier, and Y. Danto, "Long-term reliability prediction of 935 nm LEDs using failure laws and low acceleration factor ageing tests," *Quality and Reliability Engineering International*, vol. 21, no. 6, p. 571–594, Oct. 2015.
- [27] S. Chhajed, Y. Xi, T. Gessmann, J.-Q. Xi, J. Shah, J. Kim, and E. Schubert, "Junction temperature in light-emitting diodes assessed by different methods," in *Proc. SPIE on Light-Emitting Diodes: Research, Manufacturing, and Applications IX*, vol. 5739, Mar. 2005, pp. 16–24.
- [28] A. Keppens, W. Ryckaert, G. Deconinck, and P. Hanselaer, "Modeling high power light-emitting diode spectra and their variation with junction temperature," *J. Applied Physics*, vol. 108, no. 4, pp. 1–7, Aug. 2010.
- [29] F. Reifegerste and J. Lienig, "Modelling of the temperature and current dependence of LED spectra," *Journal of Light and Visual Environment*, vol. 32, no. 3, pp. 288–294, May 2008.
- [30] *Illuminance Spectrophotometer CL-500A. For evaluation of light sources including LED and EL illumination*, Konica Minolta, 2011.
- [31] Thorlabs, "PDA100A2 Si switchable gain detector – User guide," May 2019.
- [32] A. Dowhuszko, M. Ilter, and J. Hämäläinen, "Visible light communication system in presence of indirect lighting and illumination constraints," in *Proc. IEEE Int. Conf. Commun.*, June 2020, pp. 1–6.
- [33] CIE TN 001:2014, "Chromaticity difference specification for light sources," International Commission on Illumination, Technical Note., 2014.
- [34] OSRAM, "LED ColorCalculator," [Online]. Available: <https://www.osram.us/cb/tools-and-resources/applications/led-colorcalculator/index.jsp>.
- [35] K. Chickering, "Optimization of the MacAdam-modified 1965 frieze color-difference formula," *J. Opt. Soc. Am.*, vol. 57, no. 4, pp. 537–541, Apr. 1967.
- [36] —, "FMC color-difference formulas: Clarification concerning usage," *J. Opt. Soc. Am.*, vol. 61, no. 1, pp. 118–122, Jan. 1971.
- [37] D. L. MacAdam, "Visual sensitivities to color differences in daylight," *J. Opt. Soc. Am.*, vol. 32, no. 5, pp. 247–274, May 1942.